

## Degrading Mountain Permafrost in Southern Norway: Spatial and Temporal Variability of Mean Ground Temperatures, 1999–2009

Ketil Isaksen,<sup>1\*</sup> Rune Strand Ødegård,<sup>2</sup> Bernd Etzelmüller,<sup>3</sup> Christin Hilbich,<sup>4</sup> Christian Hauck,<sup>5</sup> Herman Farbrøt,<sup>3</sup> Trond Eiken,<sup>3</sup> Hans Olav Hygen<sup>1</sup> and Tobias Florian Hipp<sup>3</sup>

<sup>1</sup> Norwegian Meteorological Institute, Oslo, Norway

<sup>2</sup> Gjøvik University College, Gjøvik, Norway

<sup>3</sup> Department of Geosciences, University of Oslo, Oslo, Norway

<sup>4</sup> Department of Geography, University of Zurich, Zurich, Switzerland

<sup>5</sup> Department of Geosciences, University of Fribourg, Fribourg, Switzerland

### ABSTRACT

A ten-year record (1999–2009) of annual mean ground surface temperatures (MGSTs) and mean ground temperatures (MGTs) was analysed for 16 monitoring sites in Jotunheimen and on Dovrefjell, southern Norway. Warming has occurred at sites with cold permafrost, marginal permafrost and deep seasonal frost. Ongoing permafrost degradation is suggested both by direct temperature monitoring and indirect geophysical surveys. An increase in MGT at 6.6–9.0-m depth was observed for most sites, ranging from  $\sim 0.015$  to  $\sim 0.095^\circ\text{C a}^{-1}$ . The greatest rate of temperature increase was for sites having MGTs slightly above  $0^\circ\text{C}$ . The lowest rate of increase was for marginal permafrost sites that are affected by latent heat exchange close to  $0^\circ\text{C}$ . Increased snow depths and an increase in winter air temperatures appear to be the most important factors controlling warming observed over the ten-year period. Geophysical surveys performed in 1999 to delineate the altitudinal limit of mountain permafrost were repeated in 2009 and 2010 and indicated the degradation of some permafrost over the intervening decade.

KEY WORDS: warming permafrost; permafrost degradation; mean ground surface temperature; seasonal frost; repeated electrical resistivity tomography (ERT); long-term monitoring

### INTRODUCTION

Permafrost temperatures have risen during the last 20–30 years in almost all areas of the Arctic lowlands (e.g. Osterkamp and Romanovsky, 1999; Jorgenson *et al.*, 2006; Smith *et al.*, 2010; Romanovsky *et al.*, 2010). During the last decade, considerable attention has also been paid to rising ground temperatures in mountain permafrost and how areas with steep and cold terrain may respond to global warming (e.g. Harris *et al.*, 2009). In mountain areas, the high spatial variability of micro-climate (especially snow cover), topography, ground surface characteristics and soil-specific factors results in highly variable ground thermal regimes at a local scale. Despite significant progress in understanding these processes, the generalisation of findings to larger areas, in order to assess the dominant processes

influencing permafrost development and degradation, remains difficult (Haerberli and Gruber, 2008). The role of heat advection induced by moving water or air in coarse sediments is a further set of processes that is little understood but highly relevant for predicting permafrost response to climate change (Gruber and Haerberli, 2007).

The development of data-logging technology and especially miniature temperature dataloggers (MTDs) has greatly increased the possibilities for analysing the thermal complexity of mountain permafrost areas (cf. Hoelzle *et al.*, 1999). Combinations of geophysical and thermal monitoring approaches, such as with electrical resistivity tomography (ERT) and borehole temperature data, have been shown to be particularly suitable for long-term observation of permafrost evolution (Hauck, 2002; Hilbich *et al.*, 2009; Krautblatter and Hauck, 2007). However, these studies are generally based on a limited duration data-set since the longest continuous European permafrost temperature time series is from the Murtèl Corvatsch borehole in Switzerland which was drilled in 1987 (Vonder Mühl and Haerberli, 1990;

\* Correspondence to: K. Isaksen, Norwegian Meteorological Institute, PO Box 43, Blindern, N-0313 Oslo, Norway. E-mail: ketil.isaksen@met.no

Hoelzle *et al.*, 2002). Analysis of a comprehensive ERT-monitoring data-set from a seven-year study at Schilthorn, Swiss Alps confirmed the applicability of ERT monitoring to observations of freezing and thawing processes on short-term, seasonal and long-term scales and highlighted the impact of the hot summer of 2003 on the permafrost regime, which was more severe than previously assumed from borehole temperatures (Hilbich *et al.*, 2008).

Few observations and analyses exist from mountain areas in general on the long-term variability in mean ground surface temperature (MGST) and mean ground temperature (MGT) at a local scale. Here, we analyse a data-set based on ten years of permafrost monitoring on and around Juvvasshøe, Jotunheimen (61°40'N, 08°22'E) and on Snøheim-Hjerkin, Dovrefjell (62°15'N, 9°20'E), southern Norway (Figure 1). Data from 16 instrumented sites situated in different settings, ranging from fairly cold permafrost to marginal permafrost and non-permafrost sites with deep seasonal frost, were used to analyse the local variability and trends in MGST and MGT. In addition, ERT surveys crossing the lower altitudinal limit of permafrost, which were performed along the northeastern slope of Juvvasshøe (Figure 1) in 1999 by Hauck *et al.* (2004), were repeated in 2009 and 2010, allowing changes in subsurface characteristics to be examined. Finally, an analysis of potential factors controlling the observed variability in MGST and MGT is presented and discussed.

## STUDY AREA

The study area lies in the central and highest part of the Caledonites in southern Norway, and covers the mountain massifs of Jotunheimen and Dovrefjell (Figure 1).

During the instrumental record of air temperatures in the 20<sup>th</sup> century, there have been substantial decadal and multi-decadal temperature variations in the two study areas. A rather cold period around 1900 was followed by 'the early 20<sup>th</sup> century warming', which culminated in the 1930s. A period of cooling followed, before the recent period of warming, which has dominated most of Scandinavia since the 1960–70s (Hanssen-Bauer and Førland, 2000). The recent linear trend in annual mean air temperatures (MATs) from the nearby weather station Fokstugu (Figure 1) for the period 1970–2009 is 0.03°C a<sup>-1</sup>. For the monitoring period 1999–2009, MATs were 1–1.5°C above the 1961–90 mean annual air temperature (MAAT).

Mean precipitation (MP) on an annual basis has generally increased during the last 100 years and is now about 25 per cent higher compared to that at the beginning of the 20<sup>th</sup> century and about 15 per cent higher since 1970. For the monitoring period 1999–2009, MP was 5–10 per cent above the 1961–90 mean annual precipitation (MAP).

### Juvvasshøe Area, Jotunheimen

Permafrost research in this area started in the 1980s (e.g. King, 1984) and the first ground temperature measurements

below 5 m in Norway were measured in a 10-m deep borehole at 1851 m a.s.l. from 1982–86 (Ødegård *et al.*, 1992). MGT at 10-m depth ranged between –2.3 and –2.1°C. Based on the analysis of bottom temperature of the snow cover (BTS) data, the lower limit of possible permafrost is at about 1450 m a.s.l. (Ødegård *et al.*, 1996; Isaksen *et al.*, 2002). The mean altitudinal lapse rate of air temperature (ALRT) is calculated to be –0.005°C m<sup>-1</sup> using regression between local air temperature measurements between 1894 and 1307 m a.s.l. (Farbrot *et al.*, 2011).

At Juvvasshøe (1894 m a.s.l., Figure 1) active-layer thickness has varied between 2.0 and 2.4 m since 1999 and permafrost thickness is estimated to exceed 300 m (Isaksen *et al.*, 2007). The MAP (1961–90) is estimated to be between 800 mm a<sup>-1</sup> (Østrem *et al.*, 1988) and 1000 mm a<sup>-1</sup> (Norwegian Meteorological Institute, unpublished data) at 1900 m a.s.l. In exposed areas above 1400–1500 m a.s.l., snow cover is thin or absent until March and April due to wind erosion, with a maximum snow cover of 0.4–0.5 m in May (Ødegård *et al.*, 1992). On the east- and north-facing slopes above the present treeline at 1100 m a.s.l., snow accumulates and snow cover is more developed. Here, average snow depths based on BTS measurements performed over three winter seasons in the 1990s were 1.5 m (Isaksen *et al.*, 2002). At elevations below 1600 m a.s.l., coarse diamicton (ground moraine) dominates and the vegetation cover increases, shifting from mostly black lichens and mosses toward grass and shrubs at 1300 m a.s.l. At elevations above 1600 m a.s.l., the vegetation cover is sparse and the surface is bouldery (block field), consisting mainly of *in-situ* weathered material with blocks up to 1 m in size. The thickness of the surface sediments overlying bedrock varies from 0 m (exposed bedrock) to more than 10 m (Isaksen *et al.*, 2001; Farbrot *et al.*, 2011).

### Snøheim-Hjerkin, Dovrefjell

The lower limit of mountain permafrost on Dovrefjell, mapped using the BTS method, is about 1500 m a.s.l. (Ødegård *et al.*, 1996; Isaksen *et al.*, 2002). This limit is representative for areas with a snow cover of 1–2 m. Borehole data suggest that the transition zone of mountain permafrost begins above 1300 m a.s.l., which represents the lower limit of discontinuous mountain permafrost at exposed sites (Sollid *et al.*, 2003). Sporadic permafrost is present at elevations down to 1000 m a.s.l. in some palsa bogs (Sollid and Sørbel, 1998). The MAAT at 1505 m a.s.l. is estimated to be –2.6°C (Ødegård *et al.*, 2008) and MAP is probably about 600 mm (Østrem *et al.*, 1988). The ALRT calculated for the area using regression between air temperature measurements at 1505 m a.s.l. and Fokstugu at 972 m a.s.l. is –0.005°C m<sup>-1</sup> (Figure 1). Large flat areas are exposed to strong winds at elevations between 1400 m a.s.l. and 1600 m a.s.l. On the east-facing slopes at elevations below 1450 m a.s.l., snow accumulates and snow cover is more developed. Here, average snow depths based on BTS measurements performed over seven winter seasons in the 1990s were 1.35 m (Isaksen *et al.*, 2002). The thickness of

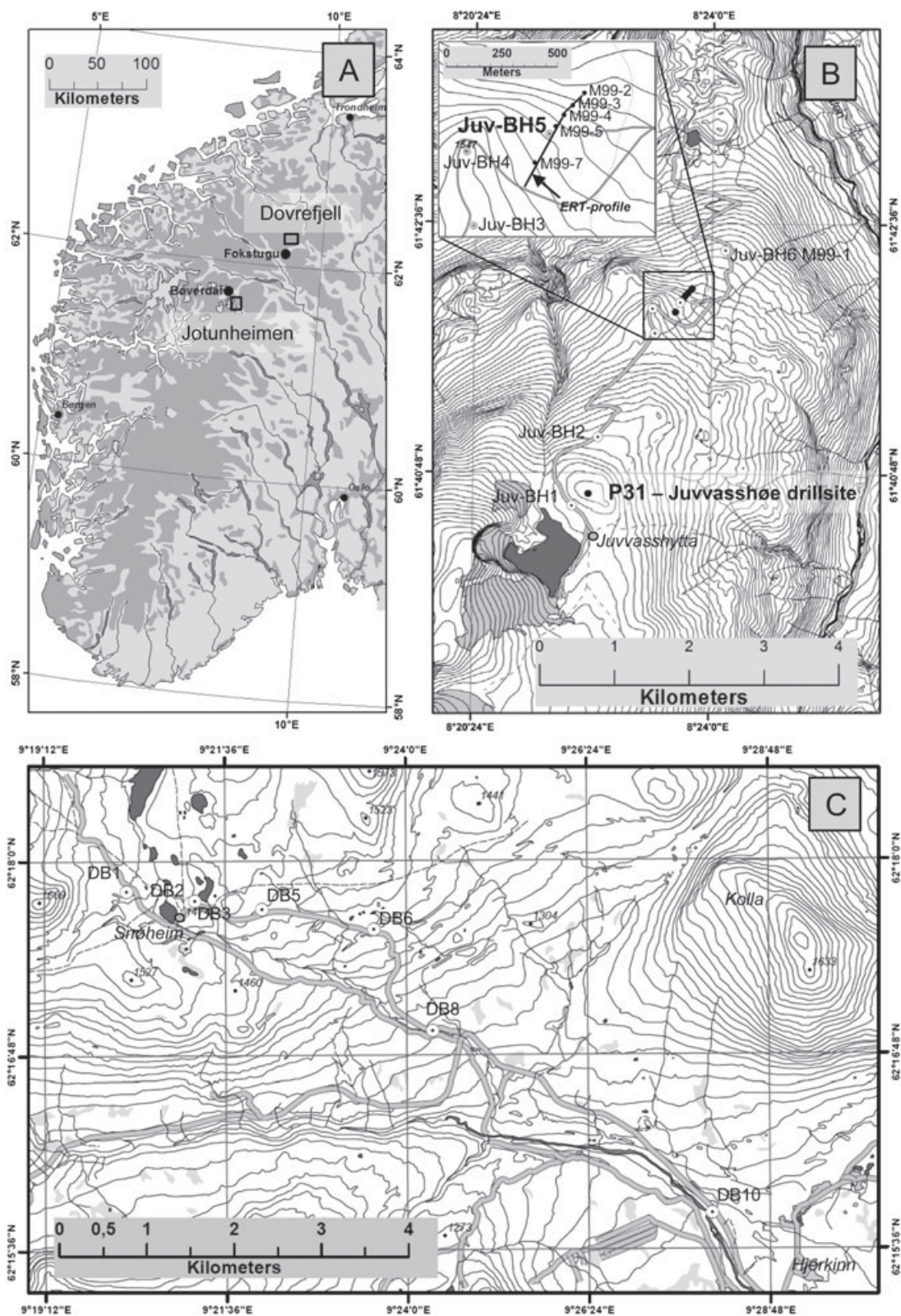


Figure 1 (A) Map of southern Norway showing the location of field sites on and around Juvvasshøe (Jotunheimen) and Snøheim-Hjerkinn (Dovrefjell). Fokstugu and Bøverdal are meteorological stations. (B) Juvvasshøe field site area: JUV-BH1 – 6 are boreholes and M99-1 – 5, 7 are miniature temperature dataloggers. Position of the electrical resistivity tomography (ERT) profile is shown in the inset map. (C) Snøheim-Hjerkinn field site: DB1 – 3, 5, 6, 8 and 10 are boreholes.

surficial materials (mainly till and glacio-fluvial deposits) varies from 0 m to more than 9 m.

## DATA AND METHODS

### Ground Temperature, Air Temperature and Wind Observations

A summary of the monitoring sites and periods is given in Table 1.

Seven MTDs, situated at different elevations and settings (Figure 1B), were installed on Juvvasshøe and along its northeastern slope in 1999. Temperatures were measured at depths of 0.1–0.2 m. The first logger site was installed at Juvvasshøe at P31 (Figure 1B) near the P30 Permafrost and Climate in Europe (PACE) borehole (cf. Sollid *et al.*, 2000). Five of the sites (M99-7, M99-5, M99-4, M99-3, M99-2) were located along the ERT profile measured in 1999 on the northeastern slope (cf. Hauck *et al.*, 2004; Figure 1B inset map). The last site, M99-1, was located at 1307 m a.s.l. within the non-permafrost zone. P31, M99-5 and M99-1 were established for long-term monitoring and have been

running since 1999, while the remaining series ended in 2003. MGST data on Snøheim-Hjerkinn were obtained from the uppermost thermistors between the surface and 0.2-m depth (see Table 1) in seven (out of 11) shallow (9 m deep) boreholes (Figure 1C). The boreholes were located along an altitudinal transect starting at 1094 m a.s.l. in deep seasonal frost and ending at 1504 m a.s.l. in discontinuous mountain permafrost (Sollid *et al.*, 2003; Ødegård *et al.*, 2008).

Ground temperature data from 1999 onwards were obtained from the 20-m deep P31 borehole on Juvvasshøe (see Figure 1B). Six more boreholes 10–15 m deep were drilled in 2008 in the Juvvasshøe area (see Farbrot *et al.*, 2011, for a full description). Data from two of these boreholes (Juv-BH5 and Juv-BH6) are used in this paper. Juv-BH5 is located close to M99-5, just within a high resistivity zone indicated by the ERT in 1999 (see Figure 7). Juv-BH6 is located at the M99-1 monitoring site. On Snøheim-Hjerkinn, ground temperature data from 2001 were obtained from the seven boreholes mentioned above.

An automatic climate station was set up 20 m from P31 in 1999 (see Isaksen *et al.*, 2003). A new official weather station was established at the same site in June 2009. Two sets of concurrent air temperature measurements have been

Table 1 Key information for monitoring sites (see Figure 1 for locations).

Site	Elev (m)	Record	Logger type	Ac, Res (°C)	TD (m)	SM	SD (m)	LT	Td (°C)
P31	1894	09.99–12.09 <sup>1</sup>	Cam <sup>a</sup>	± 0.05, 0.01	0.1–10 <sup>b</sup>	BF	< 0.2	F	0.5
Juv–BH5	1458	08.08–08.09	GeoPr	± 0.2, 0.07	0.1–10 <sup>b</sup>	M	0.2–0.8	S, Cv	1.9
Juv–BH6	1307	08.08–08.09	GeoPr	± 0.2, 0.07	0.1–9.5 <sup>b</sup>	V, M	0.2–0.8	F <sup>d</sup>	–0.3
M99–7	1480	08.99–05.03	UTL	± 0.1, 0.27	0.1	M	0.8–1.5	S	—
M99–5	1438	08.99–08.09 <sup>2</sup>	UTL	± 0.1, 0.27	0.1	M	0.2–0.8	S	—
M99–4	1430	08.99–05.03	UTL	± 0.1, 0.27	0.1	M	0.2–0.8	S	—
M99–3	1410	08.99–05.03	UTL	± 0.1, 0.27	0.1	M	> 1.5	S, Cc	—
M99–2	1391	08.99–05.03	UTL	± 0.1, 0.27	0.1	V, M	< 0.2	F, Cv	—
M99–1	1307	08.99–08.09	UTL	± 0.1, 0.27	0.1	V, M	0.2–0.8	F <sup>d</sup>	—
DB1	1505	10.01–12.09 <sup>3</sup>	Cam	± 0.08, 0.01	0.0–6.6 <sup>b</sup>	M	< 0.2	F, Cv	0.9
DB2	1481	10.01–12.09	UTL	± 0.1, 0.27	0.2, 2.0, 8.5	M	< 0.2	F, Cv	0.8
DB3	1477	10.01–12.09 <sup>4</sup>	UTL	± 0.1, 0.27	0.2, 8.5	M	> 1.5	S, Cc	–0.4
DB5	1458	10.01–12.09	UTL	± 0.1, 0.27	0.2, 8.5	M	0.2–0.8	F, Cv	1.5
DB6	1402	10.01–12.09	UTL	± 0.1, 0.27	0.2, 8.5	M	< 0.2	F, Cv	0.1
DB8	1254	10.01–12.09	UTL	± 0.1, 0.27	0.2, 8.5	B	0.2–0.8	F, Cv	1.1
DB10	1094	10.02–12.09	UTL	± 0.1, 0.27	0.2, 8.5 <sup>c</sup>	B	0.2–0.8	F, Cv	—

Note: More details about sites are found for P31 in Isaksen *et al.* (2001, 2003), Juv-BH5 and Juv-BH6 in Farbrot *et al.* (2011), M99-1 to M99-7 in Isaksen *et al.* (2002), and DB1 to DB10 in Sollid *et al.* (2003) and Ødegård *et al.* (2008).

Elev = Elevation; Logger type: Cam = Campbell (Campbell Scientific Ltd, UK); UTL = Universal Temperature Logger (Geotest AG, Switzerland); GeoPr = GeoPrecision (GeoPrecision GmbH, Germany); Ac = absolute accuracy; Res = resolution; TD = thermistor depths; SM = predominant surface material (BF = block field; M = moraine; B = bedrock; V = vegetated); SD = snow depth (average late-winter snow depth measured or estimated based on field observations, divided into four categories: < 0.2 m, 0.2–0.8 m, 0.8–1.5 m and > 1.5 m); LT = local topography within a 5–10-m radius (Cv = convex; cc = concave; F = flat; S = slope); Td = mean temperature difference between mean ground temperature (MGT) and mean ground surface temperature (MGST) at lowermost thermistor (MGT > MGST = positive).

<sup>1</sup>Data gaps for Campbell logger June–February 2007–08 and June–August 2009.

<sup>2</sup>Data gap in June–July 2003.

<sup>3</sup>Major data gap in November–February 2004–05, and some minor gaps in 2007, 2008 and 2009.

<sup>4</sup>Data are missing at 8.5-m depth between July 2005 and September 2008.

<sup>a</sup>UTL installed at 0.1-m depth.

<sup>b</sup>Thermistor chain with 11–17 thermistors.

<sup>c</sup>Temperatures observed at 8.5 m only in the first year.

<sup>d</sup>Located on a gentle slope.

made since 1999, ensuring high data quality and complete series. For wind speed and wind direction, there are data series with some minor data gaps until 2004 and 2001, respectively. In addition, wind data are available from the Fokstugu weather station. At DB1 on Snøheim, a simple climatological station with a 2-m air temperature was established in October 2001. ALRT was used to adjust air temperature to actual elevation, based on the P31 and DB1 air temperature series. Minor data gaps were filled by multiple regression analysis based on the two to three most correlated loggers nearby in order to generate consistent data series of daily average temperatures for further processing.

Snow data (as snow water equivalent, SWE) were obtained from a precipitation/degree-day model operating on  $1 \times 1 \text{ km}^2$  developed for a web-based system (<http://senorge.no/>) for producing daily snow maps for Norway (Engeset *et al.*, 2004).

To identify variations in MGST and MAT, a low-pass Gaussian filter was applied (<http://cran.r-project.org>). This method ensures easier comparison between the monitoring sites as it reduces high-frequency variations of the annual mean along the time series and makes it easier to identify local maxima and minima as well as trends. For annual ground temperatures at 2-m depth and below, a simple 365-day moving-average filter was used.

Scaling factors (N-factors) between freezing degree-days in air and at ground surface ( $N_f$ -factor) and between thawing degree-days in air and at ground surface ( $N_t$ -factor) were calculated for the sites within the permafrost transition zone along the northeastern slope of Juvvasshøe (cf. Smith and Riseborough, 2002).

## ERT

Time-lapse inversion of repeated ERT surveys between August 1999 and August 2010 crossing the expected lower altitudinal limit of permafrost in Jotunheimen allowed changes in permafrost conditions to be identified. The original geophysical profiles obtained in 1999 are discussed in detail in Hauck *et al.* (2004) and Isaksen *et al.* (2002). The upper part of the original 1999 profile of this transition zone (Figure 6 in Hauck *et al.*, 2004) was repeated in August 2009, while in August 2010 nearly the whole original profile was repeated. An ABEM multi-electrode resistivity system (ABEM Instrument AB, Sweden) with electrode spacing of 2 m was employed for all the surveys. Except for minor deviations, the 2009 and 2010 profiles were conducted along the same line as in 1999.

The tomograms stem from a time-lapse inversion of the data-sets using a robust inversion method (instead of the least-squares inversion method employed in Hauck *et al.*, 2004) and a higher damping factor with depth (factor 1.2) than was reported in 2004 to reduce potential inversion artefacts at greater depths. In addition, the depth of investigation (DOI) index technique was applied to both data-sets to identify unreliable resistivity zones in the tomograms. The method is described in detail in Oldenburg and Li (1999), and the parameters used for this paper are the

same as those applied by Hilbich *et al.* (2009) for a permafrost site in the Alps. In general, a DOI index  $>0.2$  indicates zones in the tomogram that are not constrained by the measured apparent resistivity data and therefore may represent inversion artefacts (Oldenburg and Li, 1999).

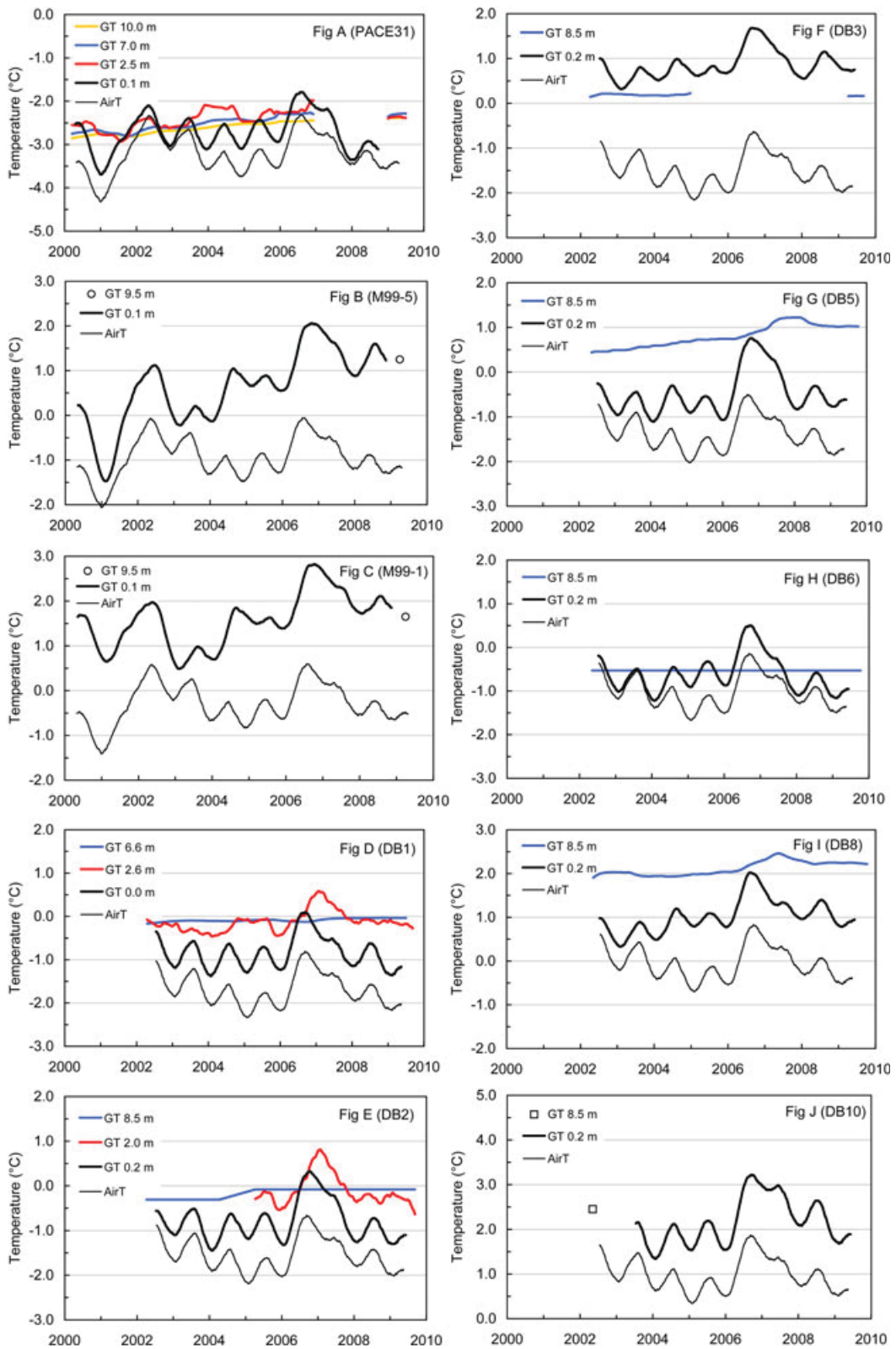
## Ground Temperature Modelling

A transient 1-D heat conduction model was used to model possible ground temperature development during the ten-year study period at Juv-BH5 (Figure 1B inset map; for details of the model see Farbroth *et al.*, 2007 and Etzelmüller *et al.*, 2011). The model accounts for latent heat and can be forced by ground surface temperature (GST) at the surface and geothermal heat flux at depth. The thermal properties of the ground are described in terms of density, thermal conductivity and heat capacity. The Juv-BH5 site has 4.5-m coarse diamicton (sandy to blocky ground moraine) over bedrock. Visual inspections during drilling of Juv-BH5 and field inspections in a nearby gravel pit suggest that the water content at present is low in sediments. For current conditions, model calibration suggests an average annual water content of  $\sim 8$  per cent by volume in sediments and  $<3$  per cent by volume in underlying bedrock. The hypothesis of a relatively dry sediment cover was also supported by the ERT data from 2009 and 2010. For the simulation, the model was first calibrated with GST values measured at Juv-BH5 between August 2008 and September 2009. The model corresponded well with measured values ( $R^2=0.99$ ). The model was then forced with the ten-year GST data-set from the nearby M99-5 (see Figure 1B inset map for location), which may have a thicker snow cover than at the top of the borehole, but is more representative for the area in a 5 – 10-m radius around the borehole. We used a constant temperature with depth as a starting condition.

## RESULTS

### Variability of Ground Temperatures and GSTs

The ten-year series of annual MGST and MAT show pronounced fluctuations, with high spatial and interannual variability within the two study areas (Figure 2). Sites P31, DB1, DB2 and DB6 are highly correlated with air temperature, while results for M99-5 and DB3, for example, indicate additional controls. All sites have their maximum GST temperatures in 2006 (Figure 2), followed by 2002 for P31, DB1, DB2, DB5 and DB6, and 2008 for M99-5, M99-1, DB3, DB8 and DB10. The ground thermal response at several of the boreholes to the warmest period in 2006 is evident from the MGTs below 2 m. At the marginal permafrost sites DB1 and DB2, the MGTs at depths of 2.0–2.5 m (within the active layer) were 0.5 to 1.0 °C higher than the previously recorded maximum values. The thermal response is also evident at 8.5-m depth for the non-permafrost sites DB5 and DB8, but with about 9–12-month delays due to the lag of the annual wave at depth.



With the exception of DB3 and Juv-BH6, the MGT observed at 8.5-m depth was higher than the corresponding MGST at 0.2-m depth (cf. Ødegård *et al.*, 2008). The mean temperature difference between 8.5-m depth and 0.2-m depth for the complete monitoring period ranged from 0.1°C at DB6 and 0.5°C at P31 to 1.9°C at Juv-BH5 and 1.5°C at DB5 (Table 1). At DB3, the MGT at 8.5-m depth was approximately 0.4°C lower than the MGST at 0.2 m.

The mean and range of annual MGST for the first four years along the northeastern slope of Juvvasshøe shows that the transect crosses from non-permafrost to permafrost (Figure 3). The range in MGST for the lowermost site M99-1 shows only positive temperatures (0.7°C to 2.4°C, with a mean of 1.4°C). The other sites fall within the range of -1.5°C (M99-2) to 2.3°C (M99-3), with means ranging from -0.6°C for M99-2 to 0.5°C for M99-3. M99-4, M99-5 and M99-7 have means close to 0°C (Figure 3).

$N_f$ -factors range from 0.83 at M99-2 to 0.34 at M99-1 (Figure 3), while  $N_t$ -values range from 1.15 at M99-5 to 0.82 at M99-3. M99-2 is an exposed site on the tread of a solifluction lobe where snow cover is thin during winter, whereas M99-1 is located on a gentle slope with low vegetation and small shrubs and where snow cover accumulates.  $N_f$  is also low at M99-3 (0.36), which has a prolonged snow cover compared to the other sites and where a depth of 3.5 m was measured in March 2000 (Isaksen *et al.*, 2002).

### Temporal Trends in Ground Temperatures and GSTs

Daily interpolated mean temperatures for P31 and DB1 are shown in Figure 4. P31 shows a typical annual temperature regime for cold mountain permafrost. Heat transfer occurs largely by conduction and the -5°C isotherm shows relatively high interannual variability in terms of depth in winter. At both sites, GSTs respond rapidly to changes in winter air temperatures. At the marginal permafrost site DB1, there is a much longer-lasting thawing period and the active layer is significantly deeper. During the warm 2006–07 autumn-winter (cf. Figure 2) the thermistor at 4.6 m did not freeze back and in 2009 the 5.6-m thermistor rose temporarily to -0.3°C and thawed for the first time in the series. The thermistor above did not respond similarly and for about one month temperatures were ~0.2°C higher at 5.6-m depth than at the 4.6-m depth. In general, the 0°C isotherm become more 'L-shaped' during thawing from 2006, with long-lasting thawing periods below 3.6 m for the last years.

Ground temperature series are shown for the sites P31, DB1 and DB5 in Figure 5. Cold permafrost is present in P31 at 9.0-m depth and pure heat conduction takes place with a stable annual amplitude of 0.7–0.9°C. The depth of zero annual amplitude is at about 16 m (Isaksen *et al.*,

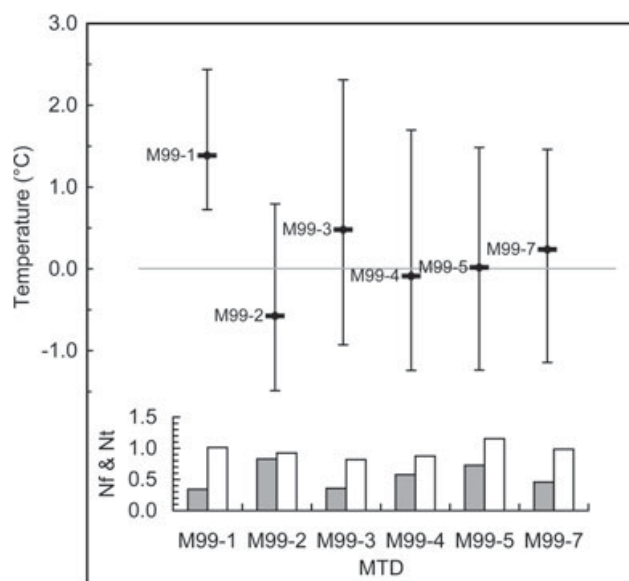


Figure 3 Mean and range of annual mean ground surface temperature for the first four years (August 1999 to May 2003) within the permafrost transition zone along the northeastern slope of Juvvasshøe.  $N_f$ -factors (grey bars show  $N_f$ , white bars show  $N_t$ ; see text for details) for the same period are shown on the lower graph. A detailed description of miniature temperature datalogger (MTD) sites M99-3 and M99-7 and analyses of the first winter 1999–2000 can be found in Figures 11 and 12 in Isaksen *et al.* (2002).

2001). In DB1 at 6.6 m, there are clear signs of annual cycling in the first four years, but from 2005 this diminishes and disappears in 2007 when temperatures stabilise between -0.1 and 0°C. In DB5 at 8.5-m depth, the MGT for the first two years was  $0.5 \pm 0.1^\circ\text{C}$  with an annual amplitude of 0.2–0.3°C. An increase in amplitude occurred from the end of 2003 and for the last four years (2007–10) the amplitude was 0.9–1.1°C. All three series showed an increase in MGT with linear trends of 0.050, -0.015 and  $\sim 0.095^\circ\text{C a}^{-1}$  for P31, DB1 and DB5, respectively, at the depths shown in Figure 5.

Warming occurred at 8.5-m depth in the other borehole series at Snøheim-Hjerkinn (Figure 2), except in DB6 which was stable at -0.5°C. DB2 showed a similar warming rate to DB1, but the DB8 non-permafrost site warmed at  $\sim 0.055^\circ\text{C a}^{-1}$ .

MGST increased at all sites between the first and last four years of available records (Figure 6). There is a significant difference in  $\Delta\text{MGST}$  between sites having thin or absent snow cover compared with those having greater snow depths. The data suggest a higher  $\Delta\text{MGST}$  for lower-lying sites compared to the highest sites (see Table 1). In addition,

Figure 2 Filtered series of mean ground temperature (GT) and mean air temperature (AirT) on an annual basis for sites in (A–C) the Juvvasshøe area and (D–G) the Snøheim-Hjerkinn area. Annual running mean GTs at selected depths are shown for the borehole sites (A and D–J). See the text for filtering techniques. In (B) and (C), mean GT at 10-m depth in boreholes Juv-BH5 and Juv-BH6, respectively, are shown as open circles for the period October 2008–September 2009. In (J), mean GT at 8.5-m depth is shown as an open square for the first-year observation period October 2001–September 2002. This figure is available in colour online at [wileyonlinelibrary.com/journal/ppp](http://wileyonlinelibrary.com/journal/ppp).

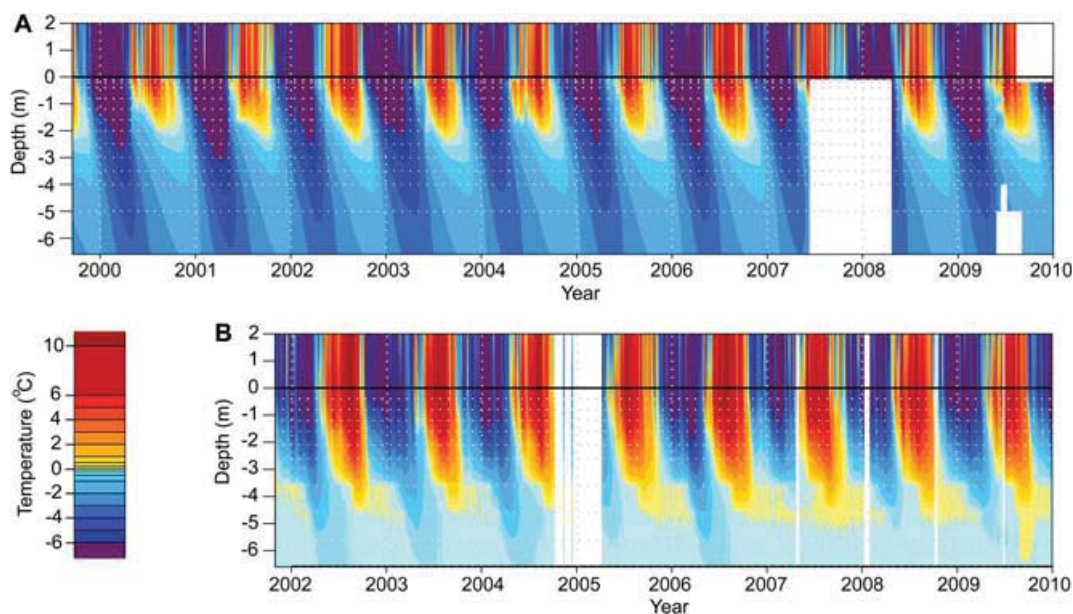


Figure 4 Daily average values of air temperatures (ATs), ground surface temperatures (GSTs) and ground temperatures (GTs) for the whole observation period for (A) borehole site P31 and (B) borehole site DB1. AT is observed at 2 m, GST in (A) is taken from miniature temperature dataloggers and GTs are taken from all borehole thermistors (grey, dotted lines) down to 6.6-m depth at both sites. In (B), the thermistor at 4.6-m depth did not freeze back in 2006–07. White/open areas are missing data. Isotherms close to 0°C are 1.0 to 0.5 to 0.2 to 0 to -0.2 to -0.5 to -1.0°C to show details during thawing and freezing. This figure is available in colour online at [wileyonlinelibrary.com/journal/ppp](http://wileyonlinelibrary.com/journal/ppp).

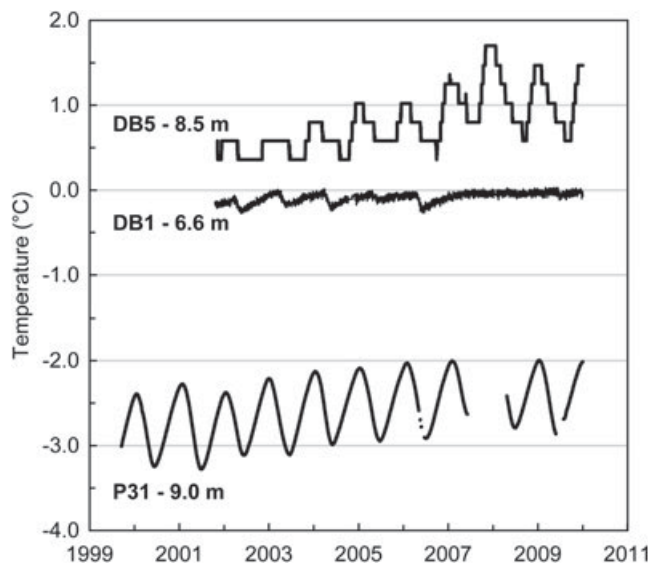


Figure 5 Daily mean temperature series for the borehole sites P31 (9.0-m depth), DB1 (6.6-m depth) and DB5 (8.5-m depth). Note the differences in data resolution and accuracy (cf. Table 1).

P31, DB1, DB2 and DB6 are located at exposed sites on main ridge crests or plateaus where snow accumulation is minimal. DB5 and DB10 are located in slightly elevated terrain and normally exhibit a thin snow cover, but have greater snow depths more than 0.5–1.0 m away from the borehole. The other sites in Figure 6 had significant snow covers during winter in most years (see Table 1).

### Changes in Electrical Resistivity in the Permafrost Transition Zone in the Juvvasshøe Area

Tomograms dating from 1999 and 2010 show high resistivities between 20 and 100 kΩm at all depths at the upper end of the Juvvasshøe profile, indicating permafrost conditions (Figure 7). However, three main changes can be discerned

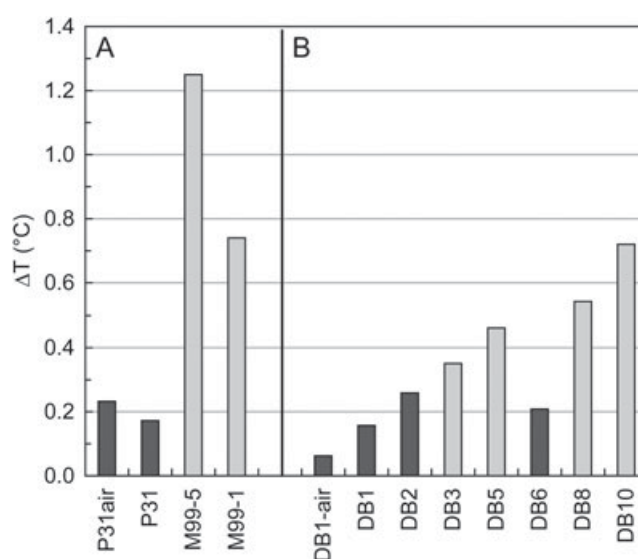


Figure 6 Temperature differences of mean ground surface temperature ( $\Delta T$ ) between (A) the four-year periods 2009–06 and 2003–00 for three sites on and around Juvvasshøe and (B) between 2009–06 and 2004–01 for the Snøheim-Hjerkinn sites. Dark bars indicate sites having thin or absent snow cover during winter; grey bars indicate sites with greater snow depths (cf. Table 1).

between the two years: (a) a strong resistivity increase in the uppermost 5–10 m of the subsurface (from values  $< 10 \text{ k}\Omega\text{m}$  to values  $> 30 \text{ k}\Omega\text{m}$ ) between 50 and 300 m along the profile; (b) a similarly strong resistivity increase at the surface between 300 and 400 m along the profile (from  $< 3 \text{ k}\Omega\text{m}$  to  $> 10 \text{ k}\Omega\text{m}$ ); and (c) a small decrease in resistivities below 5–10-m depth in zones (a) and (b) to values around  $10 \text{ k}\Omega\text{m}$ . Figure 7 (lower panel) confirms that resistivities increased more than 100 per cent at the surface between 50 and 400 m along the profile, but apparently decreased by 10–30 per cent below 5–10-m depth (e.g. red zone around the Juv-BH5 borehole). However, as this reduction occurred beneath a strong resistivity increase, the possibility of an inversion artefact cannot be excluded. Hilbich *et al.* (2009) showed that these artefacts at greater depths can be especially strong if the active layer exhibits a strong resistivity decrease, whereas they are less pronounced for resistivity increases in the active layer, as in this case. A vertical cut through both tomograms at the position of borehole Juv-BH5 shows that the resistivity increase in the uppermost 5 m is up to  $35 \text{ k}\Omega\text{m}$ , but also that the resistivity decrease below 5 m is significant ( $> 10 \text{ k}\Omega\text{m}$ ) (Figure 8C).

Annual changes from August 2009 to August 2010 (not shown) were minimal throughout the whole profile, with a slight tendency to even more resistive conditions in the uppermost 5 to 10 m in 2009. This points to a consistent resistivity pattern for these two years, and supports the observation of significant resistivity changes since 1999. The original 1999 profile was conducted after a much drier July and first week of August than in both 2009 and 2010. Based on data from the Bøverdalen station, 30-day antecedent precipitation prior to measurements in August 1999 and August 2010 totalled 35 per cent less and 65 per cent more than the 1961–90 average, respectively. The higher resistivities observed in 2010 are thus not caused by less rainfall prior to

the measurement dates, but are likely a signal of cumulative change in subsurface conditions over the preceding 11 years.

### Present Conditions and Modelled Changes in Ground Temperatures within the Transition Zone

Permafrost is not present in the Juv-BH5 borehole but seasonal frost reaches almost 4 m (Figure 8). MGT at 10-m depth was  $1.2^\circ\text{C}$ , but there was a strong offset towards the surface where MGT at 0.4 m was  $0.3^\circ\text{C}$  and  $-0.6^\circ\text{C}$  at 0.1 m. For comparison, MGST at nearby M99-5 for the same period was  $1.2^\circ\text{C}$ . In March 2009 and April 2010, snow depths were about 1 m only a few metres away from the borehole. A similar pattern was observed at DB5 and DB10.

A key question, raised from the ERT measurements and long-term GST monitoring, relates to the possible degradation of permafrost within the transition zone from approximately 1410 to 1470 m a.s.l. (cf. Hauck *et al.*, 2004). Results from transient 1-D heat conduction modelling show that with an initial value of  $0^\circ\text{C}$  the cold year 2001 could have produced short-lived permafrost, while the subsequent four warm years would have increased ground temperatures by  $0.6\text{--}0.8^\circ\text{C}$  at 10-m depth to values above  $1^\circ\text{C}$  (Figure 9). If the site had permafrost at  $-0.1^\circ\text{C}$  in 1999, the observed GST would have eliminated modelled permafrost in the upper 10 m after the warm period in 2006–07.

### Factors Influencing MGST Variability and Trends

Temperature differences between MGST and MAT (surface offset) are shown in Figure 10. For sites with significant snow covers, the surface offsets show both high temporal and spatial variability, and there are trends toward increasing values during the record. The temporal variability in the surface offset for M99-5 and M99-1 was more than  $2^\circ\text{C}$ , and for the first two

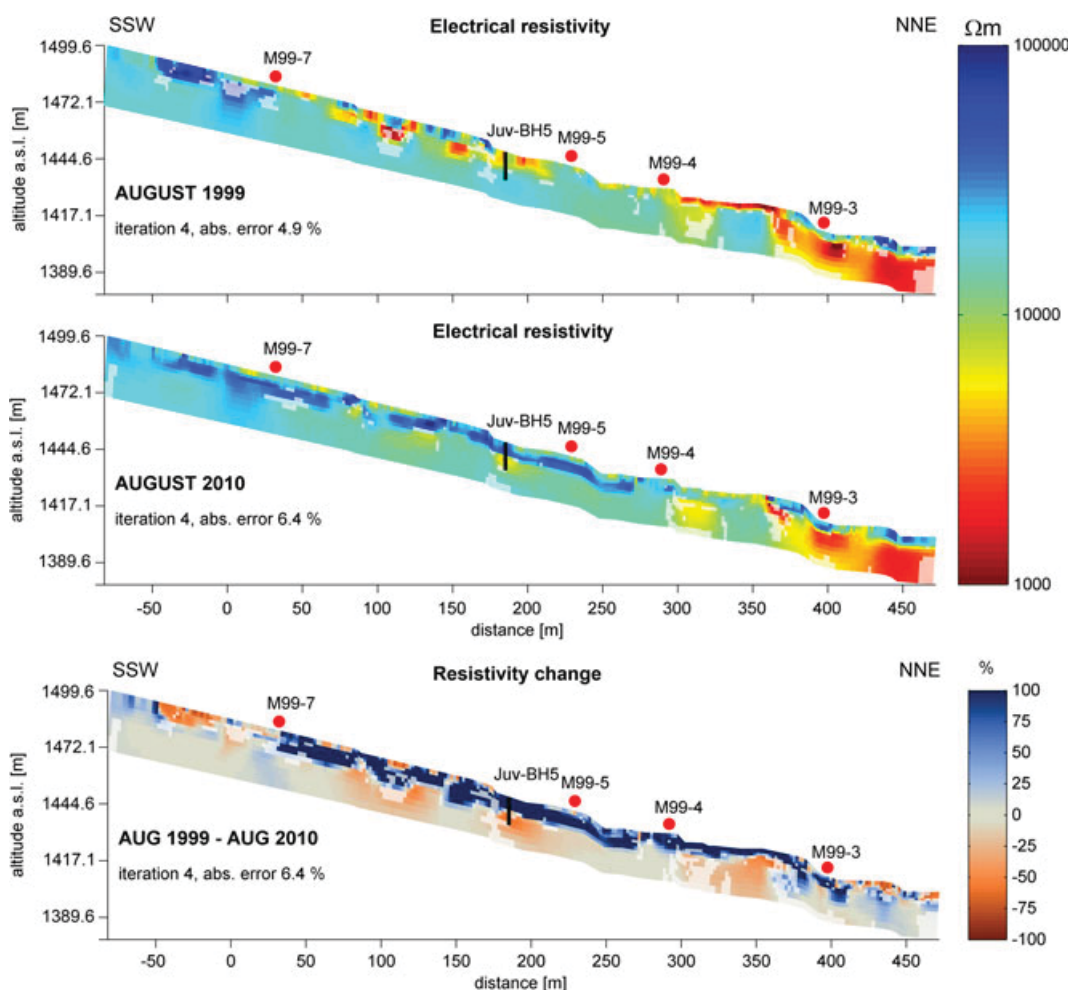


Figure 7 Time-lapse inversion of repeated electrical resistivity tomography profiles undertaken in August 1999 (upper) and August 2010 (middle) traversing the expected lower altitudinal limit of permafrost along the northeastern slope of Juvvasshøe. The lower panel shows resistivity change (%) between 1999 and 2010 along the profile. In all tomograms, the intensity of the colours was reduced in zones where the calculated depth of investigation index is  $>0.2$ , indicating unreliable inversion results. The locations of the monitoring sites M99-7, M99-5, M99-4 and M99-3 are shown, together with the 10-m deep Juv-BH5 borehole. The 1999 results are presented using a different inversion method than the one described in Hauck *et al.* (2004).

years there were great differences between the two sites. For the exposed sites (P31, DB1, DB2 and DB6) with thin or absent winter snow covers, GSTs track air temperatures, surface offsets are generally less than  $1^{\circ}\text{C}$  and temporal variability is typically  $0.5$  to  $0.8^{\circ}\text{C}$  with no clear trends through time.

The surface offset is a good indicator of the relative influence of snow versus air temperature changes on MGST. More detailed analyses of the factors influencing the variability and trend in MGST were performed for sites M99-1 and M99-5, which have the longest series and typically a snow cover of  $0.2$ – $0.8$  m (Figure 11). The analyses were confined to the winter season October – April when nearly all precipitation comes as snow at elevations above  $1300$  m a.s.l. The two sites were compared against MAT and modelled SWE, in addition to average wind speed and wind direction. Average values were used for the latter, which was possible because there is rarely wind from the north.

Results show that MGST for both sites follows interannual variability in SWE. The largest deviation was present for M99-5 in 2000–01 when MGST showed a significant response to the low MAT and a surface offset  $<0.5^{\circ}\text{C}$  similar to that observed for the exposed sites. Daily GST observations show that M99-5 was nearly free of snow in that year, as were all the other sites within the permafrost transition zone (cf. Figure 3) and they all reached their minimum MGST during that period. The exception was M99-1 where daily GST observations suggest greater snow cover. The results for the ten-year period show that MGST at M99-5 increased by  $2.0$ – $2.5^{\circ}\text{C}$ , which was significantly greater than the  $1.0$ – $1.5^{\circ}\text{C}$  increase at M99-1 (Figure 11). MAT increased by about  $0.5$ – $1.0^{\circ}\text{C}$ , while SWE increased by about  $125$ – $175$  mm. In addition, the average highest daily wind speed was considerably higher for the last four years compared to the first four

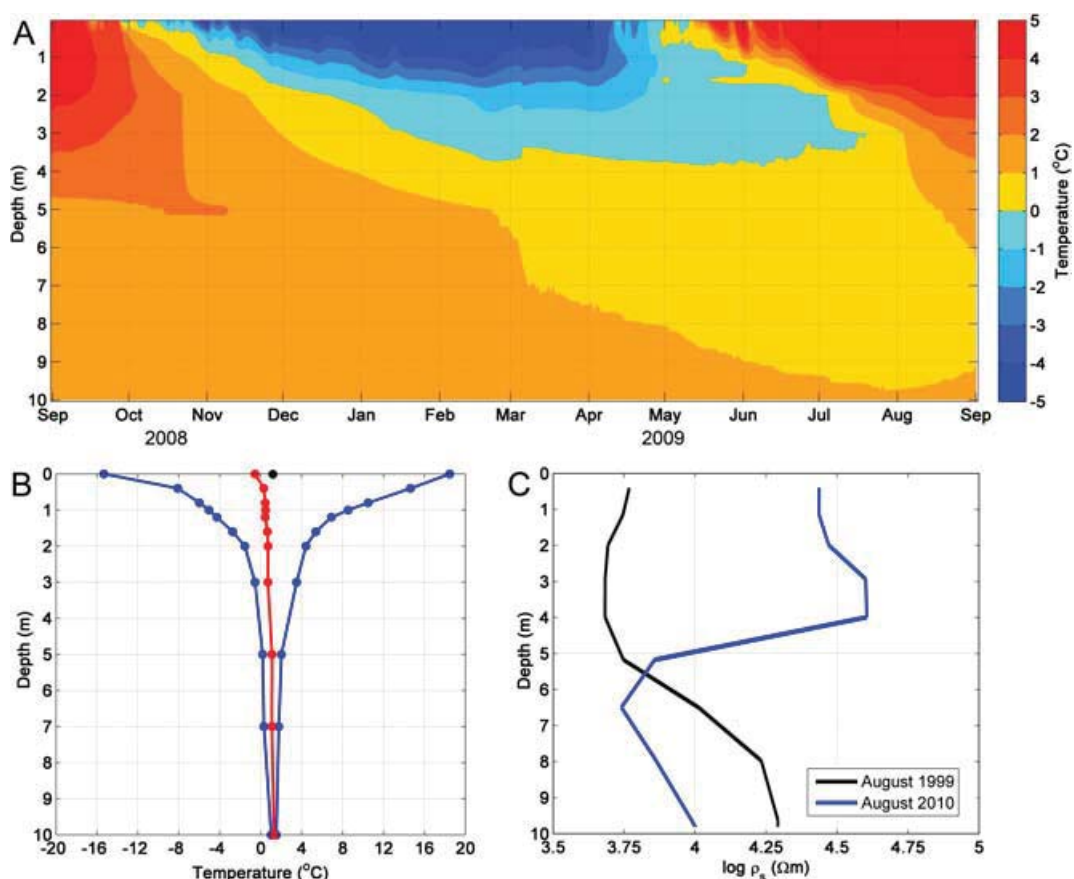


Figure 8 (A) Daily average values of ground temperatures (GTs) for Juv-BH5 between September 2008 and September 2009. Ground surface temperature is obtained from miniature temperature dataloggers and GTs are taken from all borehole thermistors down to 10-m depth. (B) Temperature envelope with mean (red line), maximum (blue line, right) and minimum (blue line, left) ground temperature profiles for the first one-year period. The black dot is the mean ground surface temperature for M99-5 for the same period. (C) Specific resistivity ( $\rho_s$ ) for the electrical resistivity tomography surveys in August 1999 and 2010 as virtual borehole through the tomograms at the position of borehole Juv-BH5 in Figure 7. This figure is available in colour online at [wileyonlinelibrary.com/journal/ppp](http://wileyonlinelibrary.com/journal/ppp).

years. This may have contributed to lower GSTs at the exposed sites due to greater scouring and higher GSTs on lee slopes due to increased re-deposition of snow by wind.

## DISCUSSION

### Variability of MGST and MGT

The results show that there is substantial spatial and temporal variability in MGST and MGT. In the Juvvasshøe area, MGST on an annual basis can vary by  $\pm 1.5$ – $2.0^\circ\text{C}$  within a distance of 30–50 m and more than  $3^\circ\text{C}$  within a distance of 100 m. This is supported by previous results (Isaksen *et al.*, 2002) which showed that 20–45 per cent of the variance in BTS can be explained by small-scale spatial variance within the 20–30 m range. In the marginal permafrost areas at Dovrefjell, differences in MGT at 8.5-m depth are  $\sim 0.6^\circ\text{C}$  within 50-m distance and when crossing the lower altitudinal permafrost limit, the difference in MGT is more than  $1.8^\circ\text{C}$  within 200 m (Sollid *et al.*, 2003; Ødegård *et al.*, 2008). At most sites, MGT at 6–10-m depth is higher than MGST

having an offset of  $0.1^\circ\text{C}$  to  $1.3^\circ\text{C}$ . At only one site was MGT at 8.5-m depth lower (by  $\sim 0.5^\circ\text{C}$ ) than MGST at 0.2 m. The same pattern is reported by Farbroth *et al.* (2011). It is thought that 3-D effects from small-scale topographic variations, leading to small-scale variations in snow depth around the boreholes, are the main reason for this offset. This is also supported by large temperature offsets observed within the upper 2–3 m in boreholes on Dovrefjell (measured manually with thermistor chains once each winter). In addition, heat advection by moving water may be important for some of the marginal and non-permafrost sites.

### Permafrost Warming and Degradation

#### *Evidence from Temperature Measurements.*

A ten-year series is quite short in a climatic context due to considerable interannual variability in temperature, precipitation, snow distribution and so on. However, previous results suggest that near-surface permafrost on Juvvasshøe has warmed by an average of  $0.04$ – $0.05^\circ\text{C a}^{-1}$  for several decades (Isaksen *et al.*, 2007) and analyses using

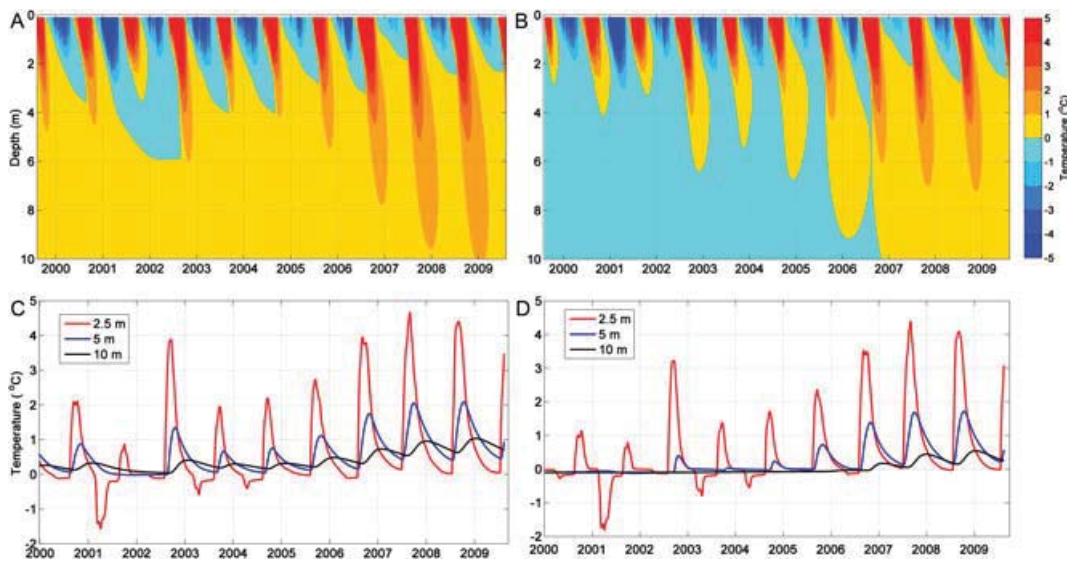


Figure 9 Transient 1-D heat conduction modelling of ground temperature (GT) calibrated for Juv-BH5 and based on input data from M99-5 during the ten-year observation period. (A) and (B) Time-depth diagrams; (C) and (D) time series for selected depths. Initialisation GT was 0 °C for (A) and (C) and -0.1 °C for (B) and (D). Average annual soil water content was estimated to be 8 per cent by volume in sediments (0–4.5 m) and below 3 per cent by volume in bedrock. This figure is available in colour online at [wileyonlinelibrary.com/journal/ppp](http://wileyonlinelibrary.com/journal/ppp).

temperatures from the 30–40-m depth show clear signs of accelerated warming in the last ten years. The changes observed at Juvvasshøe are mainly related to changes in air temperature (Isaksen *et al.*, 2007) and are representative for exposed sites with minimal snow cover.

Observations from nearby weather stations reported record-breaking temperatures in late summer, autumn and early winter 2006–07. For the one-year period July 2006–June 2007, the temperature anomaly was 2.5–3.0 °C above the 1961–90 average and was the warmest one-year period since records began in 1867 (Isaksen *et al.*, 2009). A well-preserved leather shoe found in front of a perennial ice-patch at 2000 m a.s.l. in Jotunheimen in September 2006 was dated to  $3070 \pm 40$  BP (Finstad and Vedeler, 2008), suggesting that some ice-patches in this area may have been close to their minimum extent for the last 3000 years.

The response of permafrost to the changes in GST is strongly modulated by active-layer thermal processes (e.g. Romanovsky and Osterkamp, 2000). The temperature response in the cold permafrost and relatively dry bedrock at Juvvasshøe (P31) is much greater than in, for instance, the more ice-rich unconsolidated material found at the marginal permafrost sites DB1, DB2 and DB6, where latent heat exchanges are important. The latter dampened the annual temperature amplitude and the warming signal at 8.5-m depth in DB6 (Figure 2) to below the 0.27 °C resolution of the logger (see Table 1).

Observations from DB1 showed longer-lasting thawing periods and greater thaw depths at the end of the series (Figure 4). In addition, the thermal response to the high MAT and MGST recorded in 2006–07 resulted in the first signs of talik formation between 4.5 and 5.0-m depth.

The logger accuracy at DB1 is  $\pm 0.08$  °C (Table 1) and there is 1-m spacing between the thermistors below depths of 2.6 m at the site (which may be too coarse to achieve proper resolution of the maximum thaw depth). Despite these limitations, we suggest that the ‘L-shaped’ 0 °C isotherm and the long-lasting thawing periods seen after 2006 below 3.6 m are early signs of permafrost degradation in the ice-sand-boulder mixture in the moraine found at DB1. This was also supported by a temporary thaw observed in 2009 at 5.6-m depth but which was not recognised at 4.6 and 6.6 m, which suggests heat advection and a first sign of opening up of talik/water systems (Figure 4).

DB5 on Dovrefjell is a key site for how ground temperatures may respond in a late phase of permafrost degradation, and is the first monitoring site in Norway where thermal conditions are inferred to be being observed just after thawing. Similar to DB1 and DB6, latent heat exchanges appear to dominate the annual temperature amplitude at 8.5-m depth at DB5 in the beginning of the series (Figure 5). However temperatures are above 0 °C and MGT for the two first years is  $0.5 \pm 0.1$  °C. We suggest that the increase in temperature amplitude observed at DB5 is due to gradual thawing of ice in the vicinity of the borehole (e.g. just beside or below), leading to a drier near-surface layer and thus to changes in near-surface heat exchange. The linear temperature trend observed at 8.5 m is nearly  $+0.1$  °C a<sup>-1</sup> and the highest among all the monitoring sites in this study.

#### *Evidence from the Repeated ERT.*

Using conductivity (with a Geonics EM-31 instrument (Geonics Limited, Canada)) and BTS measurements, Hauck *et al.* (2004) found that the altitudinal limit of permafrost

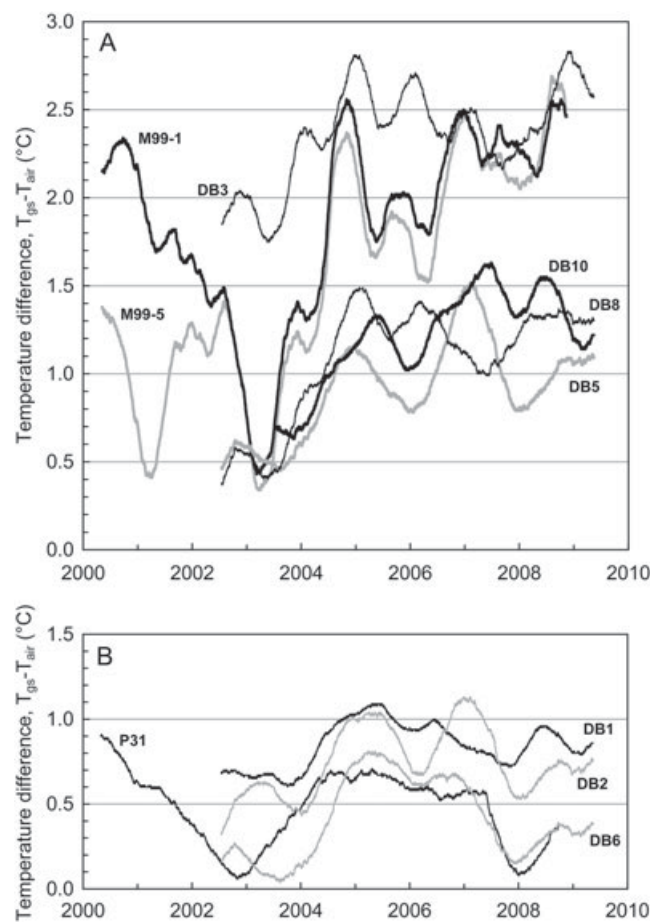


Figure 10 Temperature differences between annual mean ground surface temperature ( $T_{gs}$ ) and mean air temperature ( $T_{air}$ ) during the observation period for (A) sites with late-winter snow cover thicker than 0.2–0.8 m and (B) sites with a thin or absent snow cover during winter (cf. Figure 6). Note the differences between M99-1 and M99-5 in 2000–01 (cf. Figure 11).

along the northeastern slope of Juvvashøe could be narrowed down to elevations between about 1380 m a.s.l. and 1500 m a.s.l. Using small-scale geophysical surveys (ERT and seismics), this transition zone was further reduced to an absence of permafrost below 1410 m a.s.l. and discontinuous permafrost at elevations around 1470 m a.s.l. Between these two elevations, resistivities below the uppermost 5 m were homogeneously around 10 k $\Omega$ m, which was designated as the transition value between permafrost and non-permafrost conditions with temperatures probably around freezing point. A definite answer as to whether permafrost was present or absent in this transition zone could not be given because: (a) measured seismic P-wave velocities showed values around 3000–4000 m/s (indicating ground ice or bedrock) but also >4500 m/s (indicating bedrock) below the active layer, and (b) BTS measurements in part of this zone could not be evaluated due to shallow snow cover at the time of the measurements (Isaksen *et al.*, 2002). Nevertheless, the variable but high P-wave velocities (3000–6000 m/s) in comparison with much lower velocities at non-permafrost sites suggested at least a partially frozen subsurface (Hauck *et al.*, 2004).

Assuming that all zones in the inverted tomograms of Figure 7 not affected by increased DOI values are reliable, both the resistivity increase at the surface and the resistivity decrease below 5–10-m depth can be interpreted in the context of permafrost degradation, as suggested by the temperature data and the absence of permafrost in borehole Juv-BH5 (cf. Figure 8). First, hypothetical permafrost degradation since 1999 could have led to a resistivity decrease below the active layer due to the melting of ice. Second, decreasing ice content below the active layer could induce a resistivity increase near the surface, because a drier near-surface layer would evolve due to rapid drainage of infiltrating water through the now unfrozen and thus hydraulically conductive layer (cf. Bense *et al.*, 2009).

In contrast to the near-surface layer, the material at 5–15-m depth may not yet have dried out due to more recent permafrost degradation and possible changes in hydrological conditions, or different material properties with higher water retention capacity. The latter hypothesis is supported by the fact that bedrock was encountered at 4.5-m depth during drilling of the Juv-BH5 borehole. Melt of ice in the pores of the bedrock may have resulted in wet and thus

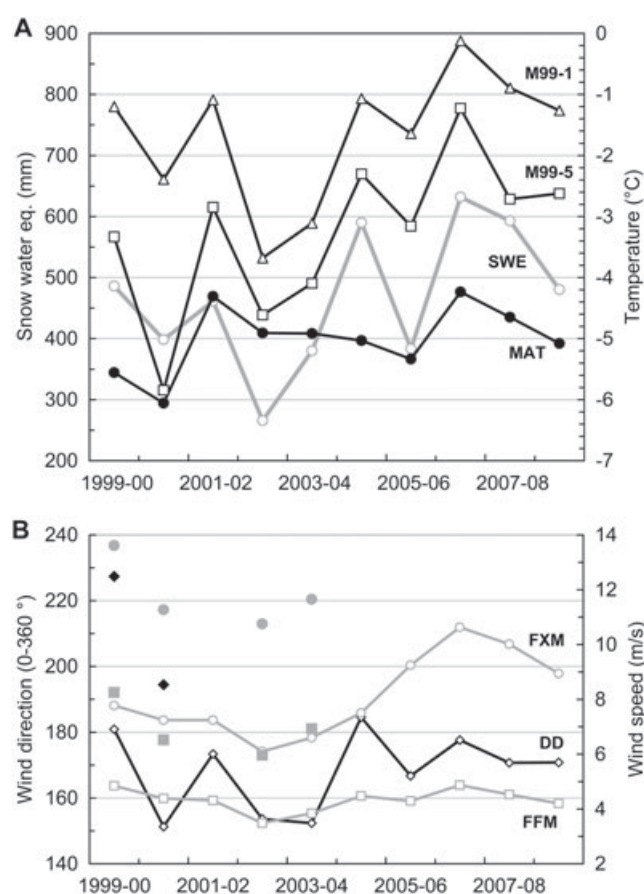


Figure 11 Comparison of variability in air temperature, snow cover, wind pattern and observed ground surface temperature. (A) Modelled mean snow water equivalent (SWE: grey line, open circles) plotted against mean air temperature (MAT; black line, filled circles) and mean ground surface temperature for October to April for sites M99-1 (black line, open triangle) and M99-5 (black line, open square). SWE and MAT were adjusted to the elevation of M99-5. (B) Observed mean wind direction and wind speed for October to April for Fokstugu and Juvvasshøe weather stations. Wind direction (DD) on Fokstugu is shown as a black line with open diamonds while on Juvvasshøe it is shown with filled diamonds (without a line). For wind speed, both average wind speed (FFM: grey line, open squares for Fokstugu; filled squares for Juvvasshøe) and the average highest mean wind values (FXM: grey line, open circles for Fokstugu; filled circles for Juvvasshøe) are shown.

less resistive bedrock, while meltwater from ice in the coarse-grained morainic material above would be able to drain, thus causing a resistivity increase compared to the warm permafrost conditions existing before thaw.

The resistivity increase at the surface observed between 300 and 400 m along the profile may point to a comparable process: a formerly impermeable layer at around 5-m depth (i.e. bedrock or frozen sediments) might have caused saturated conditions at the surface. The resistivity increase during the last 11 years may be caused by a reduced water supply from further upslope (due to improved infiltration as discussed above) and/or by thawing of formerly frozen sediments at greater depth and corresponding infiltration and thus desaturation of the surface layer. The latter hypothesis is supported by the observed resistivity decrease at greater depth. The differences in resistivities between this zone and the zone further above are most likely due to different subsurface materials: between 50 and 300 m along the profile it is thought that the material is more porous

(with higher hydraulic conductivity) at the surface than further downslope, leading to higher water saturations between 300 and 400 m in both 1999 and 2010. In addition, the lowermost (and low resistive) part of the ERT profile, which was thought to be definitively non-permafrost in 1999 (Hauck *et al.*, 2004), shows increased resistivity below 5-m depth in 2010, supporting the hypothesis of a reduced water supply from the slope above.

The unchanged resistivity values at greater depths in the uppermost part of the ERT profile suggest still-frozen conditions. Permafrost degradation would have been expected to start around the altitudinal limit in 1999 and then progress to higher elevations. The distinct resistivity decrease at the surface in this uppermost part of the profile could be a first sign of degradation as the resulting meltwater cannot drain at present. It should be noted, however, that the 1999 ERT profile was conducted after a much drier period than in 2010 when strong rain events preceded the measurements.

### *Implications from the Heat Flow Modelling.*

The short time available for calibration of the model against observations in Juv-BH5, possible effects of heat advection related to groundwater and changes in ice-water content during permafrost degradation make the results from thermal modelling somewhat uncertain. However, the rapid formation of a talik in the model within the last three years strengthens the hypothesis of permafrost degradation since 1999. In addition, if permafrost was present in 1999, the results suggest that heat advection by moving water could have been an additional factor in order to reach the present 10 m MGT of  $\sim 1.2^\circ\text{C}$ .

Observations from M99-5 suggest significant warming during the ten-year series. As observed in DB5 (Figure 5), for example, ground temperatures may respond rapidly after permafrost degradation, and at 8.5-m depth ground temperatures are currently increasing by nearly  $1^\circ\text{C}$  per decade. The observed change in MGST at M99-5 is even greater than at DB5 (Figure 6). Thus similar and even greater warming in the permafrost transition zone near Juvvasshøe could be expected, and a rise in MGT at 10-m depth of  $\sim 1.2^\circ\text{C}$  since 1999 does not appear unrealistic.

### **Controlling Factors and Relevance**

Variable snow cover appears responsible for most of interannual variability and the observed warming trend in ground temperatures (cf. Goodrich, 1982; Vonder Mühl *et al.*, 1998). Heterogeneous snow distribution in alpine terrain is the result of wind and precipitation interacting with the (snow) surface over topography (Lehning *et al.*, 2008). Modelling suggests that snow distribution on the ridge scale is primarily caused by preferential deposition. The thin snow cover during 2000–01 at M99-5 and the other logger sites on the same slope probably reflects the prevailing wind direction, which was significantly different in 2000–01 compared to 1999–2000 (Figure 11). The nearly southerly winds in 2000–01 resulted in stronger wind deflation along the northeast-facing slope than at M99-1, which is more protected. Results are also supported by a simple snow drift model (cf. Stocker Mittaz *et al.*, 2002) that estimates possible differences in snow redistribution over the permafrost transition slope and indicates more snow deflation in 2000–01 than for previous and later years when southwesterly winds prevailed.

The 3-D effects due to snow variability at marginal and non-permafrost sites in this study resulted in direct thermal responses in the near-surface layers. At greater depths, however, the average snow depth becomes more important because of the smoothing of the subsurface temperature field. The influence of individual snow-specific and climatic factors on the ground thermal regime was investigated by Luetsch *et al.* (2008) using a numerical model. The results suggest that snow depth is the most important factor for permafrost temperatures. Snow depths below a threshold value of 0.6 m lack sufficient insulation to prevent low atmospheric temperatures from cooling the soil. From field investigations, a snow depth of more than 0.6–0.8 m has

been found to be effective in thermally insulating the ground from the atmosphere (Haeberli, 1973; Keller and Gubler, 1993; Hanson and Hoelzle, 2004).

As shown in Figure 6, there is a clear elevation dependency in changes to MGST over the ten-year series. Effects of changes in snow amount as SWE (Figure 11) seem to be the most important factor, followed by the increase in winter air temperatures. In addition, wind drift strongly influences the snow accumulation pattern locally within the two study areas. Changes in wind pattern, as seen in 2000–01 (cf. Figure 11), may therefore also affect interannual variability in MGST. Our results suggest that sites that normally have snow depths around 0.2–0.8 m (e.g. M99-5 and M99-1) may have MGST and MGT values that are the most sensitive to changes in snow cover. Variability in snow depths has a lesser influence on sites with a thick snow cover (i.e.  $> 1.5$  m), and for sites exposed to strong winds and hence a thin or no snow cover, it is mainly changes in air temperature that are the dominant factor. At DB3, which is the site with the largest snow drift and thickest snow cover, changes in MGST were smaller compared to the other sites.

This study demonstrates the need to better understand how changes in winter precipitation/snow at high elevation will be altered in a warmer world (cf. Stieglitz *et al.*, 2003). The effect of different snow parameters on ground temperatures needs to be quantified, in order to improve our understanding of permafrost development under the influence of snow cover variations and/or changing climatic conditions.

### **CONCLUSIONS**

Warming occurred in two mountain massifs in southern Norway between 1999 and 2009 at sites with cold permafrost, marginal permafrost and deep seasonal frost. The combined findings from direct temperature measurements and repeated ERT indicate that permafrost degradation is occurring. The main findings are:

- An increase in MGT at 6–9-m depth occurred at most sites, with rates ranging from  $\sim 0.015$  to  $\sim 0.095^\circ\text{C a}^{-1}$ . The greatest increases in MGT were observed at sites with ground temperatures slightly above  $0^\circ\text{C}$  where permafrost may have recently degraded. At one site with ground temperatures slightly above  $0^\circ\text{C}$ , there was a significant increase in both annual amplitude and absolute temperature, which suggests gradual thawing of ice in the vicinity, leading to a drier near-surface layer and thus changes in near-surface heat exchange. The smallest MGT increase was observed at sites in marginal permafrost, where MGTs are within a few tenths of a degree below  $0^\circ\text{C}$  and are strongly modulated by latent heat exchange.
- Analyses of observed changes ( $\Delta T$ ) in MGST suggest the highest  $\Delta T$  for lower-lying sites located in marginal permafrost and deep seasonal frost with a snow cover of 0.2–0.8 m in late winter. There, increased snow depths appear to be the most important factor for the observed

$\Delta T$ , followed by an increase in winter air temperatures. For the higher elevations exposed to strong winds, where permafrost is widespread, increases in winter air temperature are the most important controlling factor. Increased snow depths over the last few years are due to greater winter precipitation and/or changes in the redistribution pattern of snow by wind.

- For most sites, MGST varies by 1.5–3.0°C over distances of just 30–100 m. Except for two sites, MGT at 6–10-m depth is generally higher than MGST with offsets of 0.1 °C to 1.9°C, possibly the result of 3-D effects from small-scale topographic variations, leading to increased snow depth around the borehole. In addition, heat advection by moving water may be important for some of the marginal and non-permafrost sites.
- The repeated ERT profiles show a substantial increase in resistivity of the upper surface layers and a decrease below 5–10-m depth: changes that are interpreted as indicating degradation of a permafrost layer that was present in 1999. The overall resistivity increase in the near-surface layer is thought to indicate drier conditions due to rapid drainage of infiltrating water through hydraulically conductive morainic material, compared to moister conditions during possible permafrost degradation in 1999. No resistivity changes were observed at greater depths in the uppermost high resistive part of the

profile, which indicates unchanged conditions during the past ten years and that permafrost is still present.

## ACKNOWLEDGEMENTS

This study was supported by the Norwegian Meteorological Institute, Gjøvik University College and the Department of Geosciences, University of Oslo. In addition, the projects CRYOLINK (185987/v30, period 2007–11) and PACE (contract ENV4-CT97-0492, period 1997–2001), financed by the Norwegian Research Council and the European Community (through the 4<sup>th</sup> Framework), respectively, gave support. Prof. em. C. Harris was coordinator of the PACE project. The opportunity he offered to participate in this project enabled the international collaboration presented here and the inspiration for our study. The long-term monitoring programme (started in 2001) on Snøheim-Hjerkinn was initiated by Prof. em. J. L. Sollid, University of Oslo. Mr O. E. Martinsen, Forsvarsbygg (The Norwegian Defence Estates Agency) partly financed the borehole drillings on the Dovrefjell operation and assisted in organising the fieldwork. M. Bathen and C. Pellet assisted in the field. The Editor and two anonymous reviewers provided important improvements to the manuscript. The contribution of all persons and institutions mentioned is gratefully acknowledged.

## REFERENCES

- Bense VF, Ferguson G, Kooi H. 2009. Evolution of shallow groundwater flow systems in areas of degrading permafrost. *Geophysical Research Letters* **36**: L22401. DOI: 10.1029/2009GL039225
- Engeset R, Tveito OE, Alfnes E, Mengistu Z, Udnæs H-C, Isaksen K, Førland EJ. 2004. Snow map system for Norway. 23<sup>rd</sup>. In *Proceedings of XXIII Nordic Hydrological Conference 2004*, Vol. 1, 8–12 August 2004, Tallinn Estonia, Jarvet A (ed.), Nordic Hydrological Programme (NHP) Report No. 51, Tartu, Tartu University Press: 112–121.
- Etzelmüller B, Schuler TV, Isaksen K, Christiansen HH, Farbrot H, Benestad R. 2011. Modeling the temperature evolution of Svalbard permafrost during the 20th and 21st century. *The Cryosphere* **5**: 67–79. DOI: 10.5194/tc-5-67-2011
- Farbrot H, Etzelmüller B, Schuler TV, Guðmundsson Á, Eiken T, Humlum O, Björnsson H. 2007. Thermal characteristics and climate change impact of mountain permafrost in Iceland. *Journal of Geophysical Research* **112**: F03S90. DOI: 10.1029/2006JF000541
- Farbrot H, Hipp T, Etzelmüller B, Isaksen K, Ødegård RS, Schuler TV, Humlum O. 2011. Air and ground temperature variations observed along elevation and continentality gradients in Southern Norway. In Press.
- Permafrost and Periglacial Processes*. DOI: 10.1002/ppp733
- Finstad E, Vedeler M. 2008. A Bronze age shoe from Jotunheimen (in Norwegian). *Viking* **LXXI**: 61–70.
- Goodrich LE. 1982. The influence of snow cover on the ground thermal regime. *Canadian Geotechnical Journal* **19**: 421–432.
- Gruber S, Haeberli W. 2007. Permafrost in steep bedrock slopes and its temperature-related destabilization following climate change. *Journal of Geophysical Research* **112**: F02S18. DOI: 10.1029/2006JF000547
- Haeberli W. 1973. Die Basis Temperatur der winterlichen Schneedecke als möglicher Indikator für die Verbreitung von Permafrost in den Alpen. [http://imgi.uibk.ac.at/iceclim/ZfG\\_Zeitschrift\\_für\\_Gletscherkunde\\_und\\_Glazialgeologie](http://imgi.uibk.ac.at/iceclim/ZfG_Zeitschrift_für_Gletscherkunde_und_Glazialgeologie) **9**: 221–227.
- Haeberli W, Gruber S. 2008. Research challenges for permafrost in steep and cold terrain: an Alpine perspective. Plenary paper. In *Proceedings Ninth International Conference on Permafrost*, Vol. 1, 29 June–3 July, Fairbanks Alaska, Kane DL, Hinkel KM (eds). Institute of Northern Engineering, University of Alaska Fairbanks: 597–605.
- Hanson S, Hoelzle M. 2004. The thermal regime of the active layer at the Murtel rock glacier based on data from 2002. *Permafrost and Periglacial Processes* **15**: 273–282. DOI: 10.1002/ppp.499
- Hanssen-Bauer I, Førland EJ. 2000. Temperature and precipitation variations in Norway 1900–1994 and their links to atmospheric circulation. *International Journal of Climatology* **20**: 1693–1708.
- Harris C, Arenson LU, Christiansen HH, Etzelmüller B, Frauenfelder R, Gruber S, Haeberli W, Hauck C, Hölzle M, Humlum O, Isaksen K, Käab A, Kern-Lütschg MA, Lehning M, Matsuoka N, Murton JB, Nötzli J, Phillips M, Ross N, Seppälä M, Springman SM, Vonder Mühll D. 2009. Permafrost and climate in Europe: Monitoring and modelling thermal, geomorphological and geotechnical responses. *Earth Science Reviews* **92**: 117–171. DOI: 10.1016/j.earscirev.2008.12.002
- Hauck C. 2002. Frozen ground monitoring using DC resistivity tomography. *Geophysical Research Letters* **29**(21): 2016. DOI: 10.1029/2002GL014995
- Hauck C, Isaksen K, Vonder Mühll D, Sollid JL. 2004. Geophysical surveys designed to delineate the altitudinal limit of mountain permafrost; an example from Jotunheimen, Norway. *Permafrost and Periglacial Processes* **15**: 191–205. DOI: 10.1002/ppp.493
- Hilbich C, Hauck C, Hoelzle M, Scherler M, Schudel L, Völksch I, Vonder Mühll D, Mäusbacher R. 2008. Monitoring mountain permafrost evolution using electrical resistivity tomography: A 7-year study of seasonal, annual, and long-term variations

- at Schilthorn, Swiss Alps. *Journal of Geophysical Research* **113**: F01S90. DOI: 10.1029/2007JF000799
- Hilbich C, Maescot L, Hauck C, Loke MH, Mäusbacher R. 2009. Applicability of Electrical Resistivity Tomography Monitoring to coarse blocky and ice-rich permafrost landforms. *Permafrost and Periglacial Processes* **20**: 269–284. DOI: 10.1002/ppp.652
- Hoelzle M, Wegmann M, Krummenacher B. 1999. Miniature temperature dataloggers for mapping and monitoring of permafrost in high mountain areas: First experience from the Swiss Alps. *Permafrost and Periglacial Processes* **10**: 113–124.
- Hoelzle M, Vonder Mühl D, Haerberli W. 2002. Thirty years of permafrost research in the Corvatsch-Furtschellas area, Eastern Swiss Alps: a review. *Norsk Geografisk Tidsskrift – Norwegian Journal of Geography* **56**: 137–145.
- Isaksen K, Holmlund P, Sollid JL, Harris C. 2001. Three deep alpine permafrost boreholes in Svalbard and Scandinavia. *Permafrost and Periglacial Processes* **12**: 13–26.
- Isaksen K, Hauck C, Gudevang E, Ødegård RS, Sollid JL. 2002. Mountain permafrost distribution on Dovrefjell and Jotunheimen, southern Norway, based on BTS and DC resistivity tomography data. *Norsk Geografisk Tidsskrift - Norwegian Journal of Geography* **56**: 122–136.
- Isaksen K, Heggem ESF, Bakkehøi S, Ødegård RS, Eiken T, Etzelmüller B, Sollid JL. 2003. Mountain permafrost and energy balance on Juvvasshøe, southern Norway. 8. In *Proceedings Volume 1, Eight International Conference on Permafrost*, Zurich, Switzerland, 21–25 July, Phillips M, Springmann SM, Arenson LU (eds.). Swets & Zeitlinger, Lisse, ISBN 9058095827: 467–472.
- Isaksen K, Sollid JL, Holmlund P, Harris C. 2007. Recent warming of mountain permafrost in Svalbard and Scandinavia. *Journal of Geophysical Research* **112**: F02S04. DOI: 10.1029/2006JF000522
- Isaksen K, Ødegård RS, Eiken T, Sollid JL. 2009. Sensitivity of mountain permafrost to extreme climatic events; a case study from the 2006–2007 air temperature anomaly in southern Norway. *Geophysical Research Abstracts*, Vol. 11, EGU2009-11457-1, 2009, 6th EGU General Assembly, Vienna Austria. Copernicus GmbH.
- Jorgenson MT, Shur YL, Pullman ER. 2006. Abrupt increase in permafrost degradation in Arctic Alaska. *Geophysical Research Letters* **33**: L02503. DOI: 10.1029/2005GL024960
- Keller F, Gubler HU. 1993. Interaction between snow cover and high mountain permafrost at Murtèl/Corvatsch, Swiss Alps. In *6<sup>th</sup> International Conference on Permafrost*, Beijing, China, Brown J, Yuanlin Z (eds.). South China University of Technology Press (Wushan Guangzhou China), ISBN 7 - 5623 - 0484 - X/P 1: 332–337.
- King L. 1984. Permafrost in Skandinavien - Untersuchungsergebnisse aus Lappland, Jotunheimen und Dovre/Rondane *Heidelberger Geographische Arbeiten* **76**: 174 pp.
- Krautblatter M, Hauck C. 2007. Electrical resistivity tomography monitoring of permafrost in solid rock walls. *Journal of Geophysical Research* **112**: F02S20. DOI: 10.1029/2006JF000546
- Lehning M, Löwe H, Ryser M, Raderschall N. 2008. Inhomogeneous precipitation distribution and snow transport in steep terrain. *Water Resources Research* **44**: W07404. DOI: 10.1029/2007WR006545
- Luetschg M, Lehning M, Haerberli W. 2008. A sensitivity study of factors influencing warm/thin permafrost in the Swiss Alps. *Journal of Glaciology* **54**: 696–704.
- Mittaz C, Imhof M, Hoelzle M, Haerberli W. 2002. Snowmelt evolution mapping using an energy balance approach over an alpine terrain. *Arctic, Antarctic, and Alpine Research* **34**: 274–281.
- Ødegård RS, Sollid JL, Liestøl O. 1992. Ground temperature measurements in mountain permafrost, Jotunheimen, southern Norway. *Permafrost and Periglacial Processes* **3**: 231–234.
- Ødegård RS, Hoelzle M, Vedel Johansen K, Sollid JL. 1996. Permafrost mapping and prospecting in Southern Norway. *Norsk Geografisk Tidsskrift - Norwegian Journal of Geography* **50**: 41–53.
- Ødegård RS, Isaksen K, Eiken T, Sollid JL. 2008. MAGST in mountain permafrost, Dovrefjell, southern Norway, 2001–2006. In *Proceedings Volume 2, Ninth International Conference on Permafrost*, University of Alaska Fairbanks, 29 June–3 July 2008, Kane DL, Hinkel KM, Institute of Northern Engineering, University of Alaska Fairbanks, ISBN 978-0-9800179-3-9: 1311–1315.
- Oldenburg DW, Li YG. 1999. Estimating depth of investigation in DC resistivity and IP surveys. *Geophysics* **64**: 403–416. DOI: 10.1190/1.1444545
- Osterkamp TE, Romanovsky VE. 1999. Evidence for warming and thawing of discontinuous permafrost in Alaska. *Permafrost and Periglacial Processes* **10**: 17–37.
- Østrem G, Dale Selvig K, Tandberg K. 1988. Atlas of the glaciers in southern Norway (in Norwegian). The Norwegian Water Resources and Energy Directorate (NVE), Hydrology Department, Report 61.
- Romanovsky VE, Osterkamp TE. 2000. Effects of unfrozen water on heat and mass transport processes in the active layer and permafrost. *Permafrost and Periglacial Processes* **11**: 219–239.
- Romanovsky VE, Drozdov DS, Oberman NG, Malkova GV, Kholodov AL, Marchenko SS, Moskalenko NG, Sergeev DO, Ukrainitseva NG, Abramov AA, Gilichinsky DA, Vasiliev AA. 2010. Thermal state of permafrost in Russia. *Permafrost and Periglacial Processes* **21**: 106–116. DOI: 10.1002/ppp.683
- Smith MW, Riseborough DW. 2002. Climate and the limits of permafrost: A zonal analysis. *Permafrost and Periglacial Processes* **13**: 1–15.
- Smith SL, Romanovsky VE, Lewkowicz AG, Burn CR, Allard M, Clow GD, Yoshikawa K, Throop J. 2010. Thermal state of permafrost in North America - A contribution to the International Polar Year. *Permafrost and Periglacial Processes* **21**: 117–135. DOI: 10.1002/ppp.690
- Sollid JL, Sørbel L. 1998. Palsa bogs as a climate indicator; examples Dovrefjell, Southern Norway. *Ambio* **27**: 287–291.
- Sollid JL, Holmlund P, Isaksen K, Harris C. 2000. Deep permafrost boreholes in western Svalbard, northern Sweden and southern Norway. *Norsk Geografisk Tidsskrift - Norwegian Journal of Geography* **54**: 186–191.
- Sollid JL, Isaksen K, Eiken T, Ødegård RS. 2003. The transition zone of mountain permafrost on Dovrefjell, southern Norway. In *Proceedings Volume 2, Eight International Conference on Permafrost*, Zurich, Switzerland, 21–25 July, Phillips M, Springmann SM, Arenson LU (eds.). Swets & Zeitlinger, Lisse, ISBN 9058095827: 1085–1090.
- Stieglitz M, Déry SJ, Romanovsky VE, Osterkamp TE. 2003. The role of snow cover in the warming of arctic permafrost. *Geophysical Research Letters* **30**: 1721. DOI: 10.1029/2003GL017337
- Vonder Mühl D, Haerberli W. 1990. Thermal characteristics of the permafrost within an active rock glacier (Murtèl/Cotvatsch, Grisons, Swiss Alps). *Journal of Glaciology* **36**: 151–158.
- Vonder Mühl D, Stucki T, Haerberli W. 1998. Borehole temperatures in Alpine permafrost; a ten year series. In *Permafrost, Seventh International Conference, Proceedings*, Yellowknife, Canada, Lewkowicz AG, Allard M (eds.), Université Laval, Centre d'études nordiques, Collection Nordicana, No 57: 1089–1095.